Reducing the Effects of Intersymbol Interference in Diffuse DPIM Optical Wireless Communications

Z. Ghassemlooy[a] , A. R. Hayes[b] and B. Wilson[a]

[a] Optical Communications Research Group, School of Engineering, Sheffield Hallam University, Pond Street, Sheffield, S1 1WB. U.K.

[b] quantumBEAM Limited, Abbey Barns, Duxford Road, Ickleton, Cambridgeshire, CB10 1SX, U.K

email: z.f.ghassemlooy@shu.ac.uk

Index Terms: Optical wireless, infrared, DPIM, digital, multipath, modulation

Abstract

This paper investigates the performance of digital pulse interval modulation (DPIM) in the presence of multipath propagation and additive white Gaussian noise. To combat intersymbol interference (ISI) guard slots and a non-linear equaliser have been introduced. The average optical power requirements (AOPR) due to ISI for cases with/without guard slots and with equaliser are analysed using a ceiling-bounce model. Results obtained show that in the absence of equalisation, DPIM without guard slot offers a lower AOPR compared with on-off keying (OOK). Introducing guard slots gives a further reduction in AOPR by up to 4 dB due to the reduced duty cycle of the DPIM signal. The performance of DPIM without guard slot buy using an equaliser is found to be significantly better than DPIM with guard slots on a channel with severe ISI.

1. Introduction

Among many different IR system configuration, the diffuse optical wireless indoor topology is the most convenient for LAN since it does not require careful alignment of the transmitter or receiver, nor does it require a LOS path to be maintained. In addition to this, it is also extremely flexible, and can be used for both infrastructure and ad hoc networks [1],[2]. However, it can incur a high optical path loss, which is typically 50 - 70 dB for a horizontal separation distance of up to 5 m [3]. The path loss is increased further if a temporary obstruction, such as a person obscure the receiver such that the main signal path is blocked; a situation referred to as shadowing. In addition a photo-detector with a wide field-of-view normally collects signals that have undergone one or more reflections from ceiling, walls and room objects. Multipath propagation causes ISI because the transmitted pulses spread out in time over alternative routes of differing lengths, limiting the maximum unequalized bit rate R_b achievable with a room volume of 10 x 10 x 3 m to typically around 16 Mbit/s [4],[5]. ISI incurs a power penalty and thus bit-error rate (BER) degradation. There are a number of modulation schemes which offer a trade-off between power requirement and BER performance. OOK is the most effective in combating ISI at low data rates (< 10 Mbps), but at high bit rates it suffers from a large power penalty [6]. Digital modulation schemes, such as PPM [7], DPIM [8], and DH-PIM [9] offer reduced power but at the expense of increased bandwidth. However, the power penalty due to ISI increases more rapidly for highly dispersive channels due to the shorter slot duration [8]. The effect of multipath propagation,

based on a ceiling bounce model (CBM), on the link performance has been widely used to predict ISI power penalties for diffuse OOK, PPM and DPIM and DH-PIM schemes [9],[10]. However, for DPIM no detailed multipath analysis employing guard slots and no previous work on equalisation to combat ISI has yet been reported. In this paper, we investigate the effectiveness of adding guard slots to each symbol and compare the results with a sub-optimum decision feedback equalization (DFE) method, which is a more conventional approach to combat the effects of ISI. Results obtained are compared with the more traditional modulation scheme such as OOK.

The remainder of this paper is organised as follows: In section 2, the optical channel model is described and parameters used to quantify the severity of ISI are defined. The unequalised DPIM systems with and without guard slots are evaluated in section 3. In section 4 the more common method of combating the effects of ISI employing some form of equalisation technique is described. In section 5, the main findings of the paper are presented and discussed. Finally, conclusions are presented in section 6.

2. Optical Channel Model

The multipath channel, described by its impulse response $h(t)$, is fixed for a given position of the transmitter, receiver and intervening reflectors, and changes significantly only when any of these are moved by distances of the order of centimetres [9]. Owing to the high bit rates and the relatively slow movement of people and objects within a room the channel will vary significantly only on a time scale covering many bit periods. It is therefore justifiable to model the channel as time invariant. The power penalties associated with the channel may be separated into two factors: optical path loss and multipath dispersion [8],[12]. The optical gain and the average received optical signal power are defined as $G_o = \int_{-\infty}^{\infty} h(t)\,dt$, and $P_{RX} = G_0 P_{TX}$, respectively, where P_{TX} is the average transmitted optical signal power. Hence, the $\text{optical path loss (dB)} = -10\log_{10} G_0$.

Here, consideration is limited to the power penalty due to multipath dispersion only. Consequently $h(t)$ is normalized to G_0 in order to give unity area as that of the ideal channel $\delta(t)$. Thus, in this case $P_{RX} = P_{TX}$, and for the remainder of this paper the average optical

power will be denoted as P_{avg}. The RMS delay spread D_{RMS} commonly used to quantify the time dispersive properties of multipath channels is given as: [13-14]:

$$D_{RMS} = \left(\int_{-\infty}^{\infty} (t-\mu)^2 h^2(t) dt \Big/ \int_{-\infty}^{\infty} h^2(t) dt \right)^{0.5}, \quad (1)$$

where μ is the mean delay, given by:

$$\mu = \int_{-\infty}^{\infty} t h^2(t)\, dt \Big/ \int_{-\infty}^{\infty} h^2(t)\, dt\,. \quad (2)$$

Practical channel measurements have shown that for diffuse configurations D_{RMS} is in the range from 1ns to 15n [14]. It has been shown that there is a systematic relationship between multipath power penalty and normalized delay spread D_T, which is a dimensionless parameter defined as D_{RMS} / bit duration T_b [14]. This relationship implies that a single parameter model is sufficient to calculate ISI power penalties, as given by the ceiling bounce model: [8],[12]

$$h(t,a) = \frac{6a^6}{(t+a)^7} u(t), \quad (3)$$

where $u(t)$ is the unit step function and $a = 11.037 \times D_{RMS}\left(h(t,a)\right)$. Equ. (3) has been used to predict multipath power penalties for OOK and PPM (unequalised and equalised), and DH-PIM (unequalised) for diffuse and non-directed LOS channels (with and without shadowing) with a high degree of accuracy. Here we investigate in detail the performance of DPIM using (3) normalized such that $G_0 = 1$, both with and without an equaliser.

3. Unequalised System

3.1 No guard slot

In DPIM each block of $\log_2 L$ data bits is mapped to one of L possible symbols, each different in length. Each symbol begins with a pulse, followed by a number of empty slots directly dependent on the decimal value of the block of data bits being encoded. The mapping of data bits to symbols for 4-DPIM using no guard slot (NGS) and one guard slot (1GS), and the equivalent DH-PIM$_2$, and 4-PPM symbols are shown in Fig. 1a. As symbol duration is variable in L-DPIM, the overall value of R_b is also variable. We therefore select the slot rate R_s such that the mean symbol duration is equal to the time taken to transmit the same number of bits using OOK or L-PPM, thus achieving the same average bit rate $\overline{R_b}$. Note, $R_S = (L_{ave} R_b) / \log_2 L$, and mean symbol length (no guard slot) $L_{avg} = 0.5(L+1)$. Figure 1b

shows the DPIM system block diagram where the encoder maps each *M*-bit OOK input bits into *L* possible DPIM(NGS) symbols. The symbols are then passed to a transmitter filter which has a unit-amplitude rectangular impulse response $p(t)$ with a duration of one slot $T_s = T_b \log_2 L / L_{avg}$ [6]. Such a slot duration gives the same $\overline{R_b}$ as OOK / PPM, assuming that all symbols are equally likely. The output of $p(t)$ is scaled by the peak transmitted optical signal power $L_{avg} P_{avg}$, and passed through $h(t)$. The received optical signal power is converted into a photocurrent by multiplying it by the photodetector responsivity *R*. Additive white Gaussian noise $n(t)$ is added to the detected signal at this point before being passed to a unit energy matched filter with an impulse response $r(t)$ matched to $p(t)$. The filter output is sampled at the end of each slot and a threshold detector then regenerates the data by assigning a "1" or "0" to each slot depending on whether the sampled signal is above or below the threshold level.

The average BER may be calculated using the method proposed in [10],[16], which is described as follows. Consider the discrete-time equivalent impulse response of the cascaded system truncated to have *j* time slots given by:

$$c_j = \begin{cases} p(t) \otimes h(t) \otimes r(t)\big|_{t=jT_s} & 1 \le j \le J \\ 0 & otherwise \end{cases}, \qquad (4)$$

where $\otimes$ denotes convolution. Unless the channel is non-dispersive, c_j contains a zero tap (with the largest magnitude) c_0, a single precursor tap and possibly multiple postcursor taps, see Fig. 2. On a non-dispersive channel the optimum sampling point, i.e. that which minimises the BER, occurs at the end of each slot. However, on dispersive channels, the optimum sampling point changes as the severity of ISI changes. In order to isolate the power penalty due to ISI, two assumptions are made:- (i) perfect timing recovery, which is achieved by shifting the time origin so as to maximise c_0 [16], and (ii) optimal decision threshold level α_{op}. Note that, since the slots are independent, identically distributed (i.i.d) different *m*-slots may have different occurrence probabilities, and when $m > 2$ the total number of valid sequences is $< 2^m$.

For a given *m*-slot DPIM denoted by b_i, let b_i be the value of the penultimate slot (PS) of that sequence, where $b_i \in \{0,1\}$. The reason why b_i in each sequence is considered can be

explained with the aid of Fig. 2. Suppose that c_j contains a zero tap, a precursor tap and 3 post cursor taps. If a transmitted sequence contains a single pulse in bit position 1, assuming that the peak output of c_j occurs in bit position 1 at the receiver, the post cursor ISI resulting from this one affects bit positions 2, 3 and 4, and the precursor ISI affects bit position 0, see case 1 of Fig. 2. Considering the P_e for bit position 4, any pulse transmitted before bit position 1 has no effect on bit position 4, see case 2. At the other extreme, the precursor ISI from a pulse transmitted in bit position 5 affects bit position 4, see case 3, but pulses transmitted in positions 6 onwards have no effect on bit position 4, see case 4. Therefore, only bits in positions 1 to 5 result in ISI which affects bit position 4. Therefore it is only necessary to consider every combination of bits 1 to 5 in order to calculate the average BER for bit position 4.

Let y_i denote the output of $r(t)$ corresponding to PS (i.e. b_i), which, in the absence of noise, is given by:

$$y_i = \left(\sqrt{\frac{E}{T_s}} \right) = L_{avg} R P_{avg} \mathbf{b}_i \otimes c_j \Big|_{j=m}, \tag{5}$$

where $E = E_b \log_2 L$ is the energy of PS, and E_b is the average energy per bit. The probability of slot error $P_{se,i}$ for the $(m\text{-}1)^{\text{th}}$ slot of sequence $\mathbf{b}_i$ is given as:

$$P_{se,i} = \begin{cases} Q\left(\dfrac{y_i - \alpha_{op}}{(\eta_0 / 2)^{0.5}} \right) & \text{if } b_i = 1 \\ Q\left(\dfrac{\alpha_{op} - y_i}{(\eta_0 / 2)^{0.5}} \right) & \text{if } b_i = 0 \end{cases} \tag{6}$$

where $\eta_o/2$ is the double-sided noise power spectral density. Using the method proposed in [15] the average probability of slot error is given by:

$$\overline{P_{se}} = \sum_{\text{all } i} p(\mathbf{b}_i) P_{se,i} \tag{7}$$

where $p(\mathbf{b}_i)$ is the probability of occurrence for a particular m-slot sequence.

Unlike PPM, where an error is confined to the symbol in which it occurs and a single slot error (SSE) can affect a maximum of $\log_2 L$ bits, in DPIM and DHPIM, having no fixed

symbol boundary format, errors are not confined to the symbols in which they occur. Thus, a SSE has the potential to affect all the remaining bits in a packet, making BER a potentially misleading measure of performance. Instead, one must consider the probability of packet error rates (PER). Using the approximation that the number of slots contained within a *D*-bit packet is $\sim L_{avg} D/\log_2 L$, $\overline{P_{se}}$ may be converted into a corresponding PER using:

$$PER \approx 1-\left(1-\overline{P_{se}}\right)^{L_{avg} D/\log_2 L} \tag{8}$$

In such pulse modulation scheme the probability of receiving a zero is greater than the probability of receiving a one. Therefore, α_{op} does not lie midway between expected "1" and "0" levels. Intuitively, since zeros are more likely, it is apparent that the probability of error P_e can be improved by using α_{op}, which is slightly higher than the midway value. This increases the probability of correctly detecting a zero, at the expense of increasing the probability of an erasure error. However, since zeros are more likely, an overall improvement in average error performance is achieved.

3.2 With guard slot

When a DPIM slot sequence is passed through a multipath channel, the postcursor ISI is most severe in the slots immediately following a pulse, see Fig. 2. From this the unique symbol structure of DPIM may be exploited to provide a simple method of improving error performance in the presence of ISI. It involves placing one or more guard slots in each symbol immediately following the pulse. Upon detection of a pulse, the following slot(s) contained within the guard slot are automatically assigned as zeros, regardless of whether or not the sampled output of $r(t)$ is above or below α_{op}. Thus, the postcursor ISI present in this slot(s) has no effect in system performance, provided that the pulse initiating the symbol is correctly detected. The inclusion of a guard slot increases the average number of slots per symbol, and consequently, in order to maintains the same average bit rate, it is necessary to reduce T_s. For DPIM with one guard slot and two guard slots, $T_s = T_b \log_2 L/L_{avg}$, where $L_{avg} = (L+3)/2$ and $(L+5)/2$, respectively. On its own a reduction in T_s would result in increased AOPR, since the ISI would affect a greater number of slots. Therefore, in order for the guard slot to achieve a net reduction in AOPR the reduction in power due to the presence of the guard slot must outweigh the increase in power due to the reduced T_s.

For DPIM(1GS), P_e for any given slot is dependent not only on the sampled signal value corresponding to that particular slot, but also on the sampled value of the previous slot. Thus, when evaluating DPIM(1GS), if c_i has m taps it is necessary to generate sequences of length (m+1) and evaluate $P_{se,m}$ for the m^{th} slot using sample values for the m^{th} and (m-1)$^{\text{th}}$ time slots. Note that by including 1GS, for a sequence length of (m+1) slots, not all the 2^{m+1} possible DPIM(NGS) sequences are actually valid, since use of a guard slot excludes all sequences which contain adjacent pulses. The guard slot does, however, increase the maximum run length of consecutive zeros. In order to explain the function of the guard slot the following notation is used. Let b_m and b_{m-1} represent the values of the m^{th} and (m-1)$^{\text{th}}$ slots in a DPIM(1GS) sequence, respectively, where $b_m, b_{m-1} \in \{0,1\}$. Let $\hat{b}_m$ and $\hat{b}_{m-1}$ represent the estimate of b_m and b_{m-1}, respectively, after passing through $h(t)$. Let y_m and y_{m-1} be the sampled output of $r(t)$ corresponding to the m^{th} and (m-1)$^{\text{th}}$ slots. The probability of slot error for DPIM(GS) cannot easily be expressed in a concise form. Consequently, pseudo code is used. $P_{se,m}$ in the m^{th} slot of DPIM(1GS) sequence is determined as follow:

if $b_{m-1} = 1$ & $\hat{b}_{m-1} = 1$ { $b_m = 0$ *and set* $\hat{b}_m$ *is set to* 0}
  $P_{se,m} = 0$
elseif $b_{m-1} = 1$ & $\hat{b}_{m-1} = 0$ { $b_m = 0$ *but* $\hat{b}_m$ *is not set to* 0}
  $P_{se,m} = Q\left(\left(\alpha_{op} - y_m\right) \Big/ \sqrt{\eta_0 / 2}\right)$
elseif $b_{m-1} = 0$ & $\hat{b}_{m-1} = 0$ { b_m *could be* 1 *or* 0 }
  if $b_m = 1$
    $P_{se,m} = Q\left(\left(y_m - \alpha_{op}\right) \Big/ \sqrt{\eta_0 / 2}\right)$
  else
    $P_{se,m} = Q\left(\left(\alpha_{op} - y_m\right) \Big/ \sqrt{\eta_0 / 2}\right)$
  end
elseif $b_{m-1} = 0$ & $\hat{b}_{m-1} = 1$ { $\hat{b}_m$ *is set to* 0, *but* b_m *could be* 1 }
  if $b_m = 1$
    $P_{se,m} = 1$
  else $P_{se,m} = 0$
  end
end

Similarly for DPIM(2GS), let y_{m+1} be the sampled output of $r(t)$ corresponding to the (m+1)$^{\text{th}}$ slot. For any given (m+2)-slot DPIM(2GS) sequence the probability of slot error in the (m+1)$^{\text{th}}$ slot may be calculated as follows:

If $b_{m-1} = 1$ & $\hat{b}_{m-1} = 1$ { $b_{m+1} = 0$ and $\hat{b}_{m+1}$ is set to 0}

$P_{se,m+1} = 0$

elseif $b_{m-1} = 1$ & $\hat{b}_{m-1} = 0$ { $b_{m+1} = 0$ but $\hat{b}_{m+1}$ is not set to 0}

if $\hat{b}_m = 1$

$P_{se,m+1} = 0$

else

$P_{se,m+1} = Q\left(\left(\alpha_{op} - y_{m+1}\right) \Big/ \sqrt{\eta_0 / 2}\right)$

end

elseif $b_{m-1} = 0$ & $\hat{b}_{m-1} = 0$ { b_{m+1} could be 1 or 0}

if $b_m = 1$ & $\hat{b}_m = 1$ { $b_{m+1} = 0$ and $\hat{b}_{m+1}$ is set to 0}

$P_{se,m+1} = 0$

elseif $b_m = 1$ & $\hat{b}_m = 0$ { $b_{m+1} = 0$ but $\hat{b}_{m+1}$ is not set to 0}

$P_{se,m+1} = Q\left(\left(\alpha_{op} - y_{m+1}\right) \Big/ \sqrt{\eta_0 / 2}\right)$

elseif $b_m = 0$ & $\hat{b}_m = 0$ { b_{m+1} could be 1 or 0}

if $b_{m+1} = 1$

$P_{se,m+1} = Q\left(\left(y_{m+1} - \alpha_{op}\right) \Big/ \sqrt{\eta_0 / 2}\right)$

else

$P_{se,m+1} = Q\left(\left(\alpha_{op} - y_{m+1}\right) \Big/ \sqrt{\eta_0 / 2}\right)$

end

elseif $b_m = 0$ & $\hat{b}_m = 1$ { $\hat{b}_{m+1}$ is set to 0, but b_{m+1} could be 1}

if $b_{m+1} = 1$

$P_{se,m+1} = 1$

else

$P_{se,m+1} = 0$

end

end

elseif $b_{m-1} = 0$ & $\hat{b}_{m-1} = 1$ { $\hat{b}_{m+1}$ is set to 0, but b_{m+1} could be 1 }

if $b_{m+1} = 1$

$P_{se,m+1} = 1$

else

$P_{se,m+1} = 0$

end

end

4 Equalisation

In DPIM symbol boundaries are not known prior to detection, therefore practical implementation of maximum likelihood sequence detection (MLSD) to combat ISI is not feasible because of its complexity. Hence the need for equalisation for combating the effects of ISI. Here, we consider sub-optimal DFE, which is a non-linear technique offering performance and complexity intermediate between linear equaliser and MLSD [17]. The two most popular criteria that a DFE can employ to optimise its filter coefficients are zero forcing (ZF) and mean square error (MSE). In [18] it has been shown that whilst the performance of MSE-DFEs is generally superior to that of ZF-DFEs, at high signal-to-noise ratios their performance is virtually identical. Since the analysis of ZF-DFEs is more straightforward the majority of research carried out has focused on this type of DFE [19-21]. Continuing this approach, a ZF-DFE is considered exclusively in the analysis for DPIM(NGS).

The DFE consists of a feed-forward filter, normally a whitened matched filter (WMF) matched to the received pulse shape, a detector and a feedback filter, see Fig. 3. In the context of a ZF-DFE, the WMF plays an important role of equalising the precursor ISI, which is defined as the interference from future data symbols. Therefore the remaining ISI is postcursor, meaning that it is due to past data symbols. By feeding back the detected estimate of these past data symbols, the ISI they introduce on future symbols may be cancelled. This task is performed by the feedback filter, which is sometimes referred to as the postcursor equaliser.

The impulse response of the receiver filter is given by:

$$r(t) = p(-t) \otimes h(-t)\,. \tag{9}$$

The noise-whitening filter is calculated as follows. Since $r(t)$ has an impulse response which is a time reversed version of the received pulse shape, if the optimum sampling point is selected by maximising the zero tap c_0, then c_j will have an equal number of precursor and postcursor taps. Assuming that c_i has a total of $(2m+1)$ taps, then following [22], let $C(z)$ denote the two-sided z transform of c_j, i.e.,

$$C(z) = \sum_{j=-m}^{m} c_j z^{-j} \ . \tag{10}$$

The 2*m* roots of $C(z)$ have the symmetry that if ρ is a root, then $1/\rho^*$ is also a root (asterisk denoting complex conjugate). Therefore, $C(z)$ can be factored and expressed as:

$$C(z) = W(z)W^*(1/Z^*), \tag{11}$$

where $W(z)$ has *m* roots $\rho_1, \rho_2, \ldots \rho_m$ and $W^*(1/z^*)$ has *m* roots $1/\rho_1^*, 1/\rho_2^*, \ldots 1/\rho_m^*$. If all the roots of $W^*(1/z^*)$ are inside the unit circle, i.e. the filter is minimum phase, $1/W^*(1/z^*)$ represents a physically realisable, stable, recursive discrete-time noise whitening filter. This filter whitens the noise, which is coloured by $r(t)$. Let w_j denote the tap coefficients of $1/W^*(1/z^*)$. $p(t)$, $h(t)$, WMF, the scaling for the peak P_{TX}, R and P_{avg} may be expressed as a discrete-time impulse response, given by:

$$g_j = L_{avg} R P_{avg} \cdot c_j \otimes w_j, \tag{12}$$

The discrete-time output of WMF is passed to a threshold detector, which assigns a "1" or a "0" to each slot. The output of the threshold detector $\hat{\mathbf{b}}_j$ is the estimate of the transmitted slot sequence $\mathbf{b}_j$ and forms the input to a feedback filter with an impulse response $g_j - g_0\delta_j$,[22] which represents the strictly causal portion of g_j.

Assuming that all detected slots are correct, and the filters have an infinite number of taps that are optimally adjusted in accordance with the ZF criterion, P_{se} using a ZF-DFE with the threshold level set midway between expected one and zero levels is given by [23],[24]:

$$P_{se,ZF-DFE} = Q\left(0.5 g_0 / (0.5\eta_0)^{0.5}\right). \tag{13}$$

5 Results and Discussions

All optical power requirements in this section are normalized to the average optical power required by OOK, operating at a given R_b, to achieve a PER of 10^{-6} on an ideal channel $\delta(t)$, limited only by AWGN. Packet lengths are assumed to be **1 kbyte. To calculate AOPR all**

possible sequences of *m*-slot length of DPIM were generated. For each value of D_T in the range of 10^{-3} to 0.4, first the parameter a is determined from $a = 11.037 \times D_{RMS}\left(h(t,a)\right)$ and $h(t)$ is calculated using (3). c_i is then determined from (4) with the optimum sampling point and threshold level chosen to maximise c_0. From (8), we calculate $\overline{P_{se}}$ in order to achieve the target PER of 10^{-6} for all possible valid sequences. Knowing the probability of occurrence of each sequence, $P_{se,i}$ is calculated from (7). Finally from (5) the average optical power requirement is determined.

For various PERs α_{op} was determined iteratively for various orders of DPIM(NGS) and DPIM(1GS). The method used to achieve this involves making an initial estimate for P_{avg}, and then iteratively determining α_{op} and hence, the minimum PER. This value is then compared with the target PER and, if necessary, P_{avg} is adjusted and the whole process repeated until the target PER is reached. α_{op} versus PER for DPIM(NGB) and DPIM(GB) are plotted in Figs. 4a and 4b, respectively. In Fig. 4, α_{op} normalized to the expected matched filter output when a one is transmitted. From Fig. 4 it is clear that as the P_e falls, i.e. as the SNR increases, α_{op} tends towards the midway value for both DPIM(NGB) and DPIM(1GS). With the exception of moving from 2-DPIM(NGB) to 4-DPIM(NGB), it is also evident that increasing L moves α_{op} further away from the midway value.

For DPIM(GS) the normalized AOPR versus D_T are shown in Fig. 5. Also shown for comparison are the results for OOK and DPIM(NGS). At low values of D_T, adding a guard slot reduces the average duty cycle of the transmitted signal and hence gives a reduction in AOPR. This effect is more pronounced at lower orders, where the average duty cycle is reduced by a greater percentage. As D_T increases the difference between the NGB and 1GS curves increases thus highlighting the effectiveness of adding a single guard slot. At normalized delay spreads where DPIM(NGB) experiences irreducible error rates the power requirements are finite for DPIM(1GS). Adding a second guard slot gives a further reduction in power requirements at low values of D_T. Again, this is more pronounced at lower orders. For high values of D_T, the improvement in performance over 1GS is clear, with irreducible error rates occurring at higher values of D_T than they do for 1GS. However, for intermediate values of D_T, adding a second guard slot results in only a marginal reduction in power requirement. The reason for this can be explained with the aid of Fig. 6, which shows the optical power penalty (defined as the difference between the optical powers required on dispersive and non-dispersive channels) versus D_T. From Fig. 6 it may be observed that at

intermediate values of D_T ($10^{-2} < D_T < 10^{-1}$), 2GS gives a higher power penalty than 1GS. Indeed for $L = 32$, there is a region where 2GS has a higher power penalty than NGB. This means that the benefit of adding a second guard slots is outweighed by the reduction in slot duration required to accommodate it. Therefore, in these regions the power requirements of 2GS converge with those of 1GS. Even with the use of a guard slot OOK still has a lower power requirement at high values of D_T. The inclusion of a guard slot simply increases the value at which the crossover takes place. For example, considering $L = 32$, OOK offers a lower power requirement compared with NGB for $D_T > 0.13$, whilst this crossover does not take place until $D_T = 0.18$ for 1GS and $D_T = 0.31$ for 2GS.

Using (13) and converting into an average PER using (8) and substituting for $L_{avg} = (L+1)/2$, the AOPR for DPIM(NGB) using a slot-rate ZF-DFE was calculated for various orders and D_T, as plotted in Fig. 7. Also shown in Fig. 7 for comparison are the AOPRs for unequalized DPIM(NGB). At low D_T, typically below 0.01, the ZF-DFE gives no improvement in performance. However, as expected, the effectiveness of the equaliser in reducing the AOPR becomes apparent as D_T increases. For example, when $D_T = 0.1$, the ZF-DFE yields power penalty reductions of ~1 dB - 3 dB, for the orders considered. In order to compare the effectiveness of the guard slot technique, as discussed in the previous section, with the ZF-DFE, optical power requirements for both are plotted in Fig. 8 for $L = 4$ and $L = 32$. At low D_T the power requirements of DPIM(NGB) using a ZF-DFE are virtually identical to those without equalisation, and consequently DPIM with a GB outperforms the equalised scheme. However, for any given D_T, the ISI power penalty for DPIM(NGB) using a ZF-DFE is lower than it is for unequalized DPIM(NGB), DPIM(1GS) and DPIM(2GS). Consequently, as D_T increases the power requirement curves for DPIM(NGB) using a ZF-DFE intersect with those of DPIM(1GS) and DPIM(2GS). Beyond the final points of intersection DPIM(NGB) using a ZF-DFE offers the lowest AOPR of the schemes considered. However, significant improvements in performance are not achieved until D_T is high, typically above 0.3, and on channels where the ISI is not too severe, the guard slot technique incurs only a small power penalty compared with the ZF-DFE. For example, with $L = 32$ and $D_T = 0.16$ DPIM(NGB) has an irreducible error rate, whilst DPIM(1GS) results in an AOPR which is ~3.2 dB higher than that of DPIM(NGB) using a ZF-DFE. By using DPIM(2GS) this power penalty reduces to a mere ~0.4 dB compared with DPIM(NGB) using a ZF-DFE. The analysis carried out for the DPIM with ZE-DFE makes the assumptions that $h(t)$ is known *a priori*, and the filters

used in the ZF-DFE have an infinite number of taps with the tap weights perfectly adjusted. In practise, neither of these is true, and an adaptive ZF-DFE with a finite number of taps will give a performance below that of the optimum ZF-DFE used in this section. Furthermore, if the threshold detector makes an incorrect decision the ISI correction is flawed for future decisions. This phenomenon is known as error propagation and tends to result in bursts of errors. This effect has not been considered in this analysis and is currently the subject of further study.

6 Conclusions

In this paper the effect of multipath dispersion on DPIM and techniques that may be used to combat it have been analysed. Analysis for error performances (with/without eualization) have been presented and results obtained are compared with the more established technique of OOK. We have shown that on channels with severe ISI the difference in AOPR between 16-DPIM(NGB) and 16-DPIM(1GS) increases by approximately a factor 4, thus highlighting the effectiveness of a guard slot technique in this context. On majority of channels the use of a guard slot may be sufficient to achieve reliable performance over a low value of normalised delay spread. However, at high values of normalised delay spread ($D_T > 0.2$), we have shown that DPIM (NGS) using equalization give significant improvement in performance over DPIM with/without guard slots.

7 References

[1] STREET, A.M., *et -al*: “Indoor optical wireless systems – a review,” Optical and Quantum Electns., 1997, **29**, pp. 349-378

[2] GFELLER, F.R., *et -al* : “Infrared communication for in-house applications,” in Proc. of IEEE Conf. on Comp. Commun., U.S.A., 5-8 Sep. 1978, pp. 132-138

[3] KAHN, J.M., KRAUSE, W.J., and CARRUTHERS, J.B.: "Experimental characterization of non-directed indoor infrared channels", IEEE Trans. on Commun., 1995, **43** (2/3/4), pp. 1613-1623

[4] GFELLER, F.R., and BAPST, U.H.: “Wireless in-house data communication via diffuse infrared radiation,” Proc. of the IEEE, 1979, **67**(11), pp. 1474-1486

[5] SMYTH, P.P., MCCULLAGH, M., WISELY, D., WOOD, D., RITCHIE, S., EARDLEY, P. and CASSIDY,S.: "Optical wireless local area networks - enabling technologies," BT Techg. J., April 1993, **11** (2), pp. 56-64

[6] WONG, K.K., O'FARRELL, T., and KIATWEERASAKUL, M.: "The performance of optical OOL, 2-PPM and spread spectrum under the effects of multipath dispersion and artificail light interference", Int. J. Commun., Syst., 2000, **13**, pp. 551-576
[7] GHASSEMLOOY, Z., and HAYES, R.A.: "Digital pulse interval modulation for IR Communications systems, a review", Int. J. Commun. Syst., 2000, **13**, pp. 519-536
[8] CARRUTHERS, J.B., and KAHN, J.M.: “Modeling of nondirected wireless infrared channels,” IEEE Transactions on Communications, 1997, **45** (10), pp. 1260-1268
[9] ALDIBBIAT, N. M., GHASSEMLOOY, Z., and MCLAUGHLIN, R.: "Dual header pulse interval modulation for dispersive indoor optical wireless communication systems", IEE Proc. Cirs., Devs. and Sys., 2002, **148** (3), pp. 187-192
[10] HAYES, A. R., GHASSEMLOOY, Z., & SEED, N. L., "The performance of digital pulse interval modulation in the presence of multipath propagation", 2nd Intenr. Sympos. on Commun. Sys., Networks, and DSP, 2000, UK, July 2000, pp. 141- 146
[11] KAHN, J.M., BARRY, J.R., AUDEH, M.D., CARRUTHERS, J.B., KRAUSE, W.J., AND MARSH, G.W.: “Non-directed infrared links for high-capacity wireless LAN’s,” IEEE Personal Commun. Magaz., 1994, **1**, pp. 12-25
[12] CARRUTHERS, J.B., and KAHN, J.M.: “Modeling of nondirected wireless infrared channels”, IEEE Intern. Conf. on Communs., Jun 23-27 1996, USA, **2**, pp. 1227-1231
[13] RAPPAPORT, T.S.: “Wireless Communications,” Prentice-Hall, New Jersey, 1996
[14] MARSH, G.W., and KAHN, J.M.: “Performance evaluation of experimental 50-Mb/s diffuse infrared wireless link using on-off keying with decision-feedback equalization,” IEEE Trans. on Communs., 1996, **44** (11), pp. 1496-1504
[15] BARRY, J.R., KAHN, J.M., KRAUSE, W.J., LEE, E.A., and MESSERSCHMITT, D.G.: "Simulation of multipath impulse response for indoor wireless optical channels", IEEE J. Sel. Areas in Commun., 1993, **11** (3), pp. 367-379
[16] GHASSEMLOOY, Z., HAYES, A.H., SEED, L., and KALUARACHCHI, D.: "Digital pulse interval modulation for optical communications", IEEE Commun., Magz., 1998, **36** (12), pp. 95-99
[17] AUSTIN, M.E.: “Decision-feedback equalisation for digital communication over dispersive channels,” M.I.T. Lincoln Lab., Lexington, U.S.A., 1967, Tech. Report 437
[18] BELFIORE, C.A.: “Decision feedback equalization,” Proce. of the IEEE, 1979, **67** (8), pp. 1143-1156
[19] BARRY, J.R.: *Wireless Infrared Communications*. Kluwer Academic, 1994

[20] AUDEH, M.D., KAHN, J.M., and BARRY, J.R.: "Decision-feedback equalization of pulse-position modulation on measured nondirected indoor infrared channels," IEEE Trans. on Communs., 1999, **47** (4), pp. 500-503

[21] LEE, D.C., and KAHN, J.M.: "Coding and equalization for PPM on wireless infrared channels," Proce. of IEEE Global Communs. Conf., Australia, 8-12 Nov. 1998, **1**, pp. 201-206

[22] PROAKIS, J.G.: *Digital Communications*, Third Edition. McGraw-Hill, 1995

[23] SHIU, D., and KAHN, J.M.: "Differential pulse position modulation for power-efficient wireless infrared communication," Proce. of IEEE Global Commun. Conf., Australia, 8-12 November 1998, **1**, pp. 219-224

[24] SHIU, D., and KAHN, J.M.: "Differential pulse-position modulation for power-efficient optical communication," IEEE Trans. on Communs., 1999, **47** (8), pp. 1201-1210

Figure captions

Fig. 1: (a) Mapping of source data to transmitted symbols for 4-DPIM, 4-PPM, 4-DHPIM, and (b) block diagram of the unequalised DPIM(NGB) system.

Fig.1: Response of c_j to a single one in various bit positions

Fig. 3: Equivalent discrete-time block diagram of DPIM system with DFE

Fig.4: Normalized optimum threshold level versus PER, (a) DPIM(NGS), and (b) DPIM(1GS).

Fig. 5: Normalized average optical power requirement Vs. normalized delay spread for DPIM(NGS), DPIM(1GS) and DPIM(2GS) with: (a) $L = 4$, (b) $L = 8$, (c) $L = 16$, and (d) $L = 32$. Also shown is OOK.

Fig. 6. DPIM Optical power penalty Vs. normalized delay spread.

Fig. 7: Normalized average optical power requirement Vs. normalized delay spread for unequlaised DPIM(NGB) and with a ZF-DFE

Fig. 8: Normalized average optical power requirement Vs. normalized delay spread for DPIM(NGS), DPIM(1GS), DPIM(2GS) and DPIM(NGS) with a ZF-DFE for $L = 4$ and $L = 32$

Input data	4-DPIM (NGS) Symbols	4-DPIM (1GS) symbols	DH-PIM$_2$ symbols	4-PPM symbols
00			2GS	
01		1GS		
10	T_s		1GS	
11	Information			

(a)

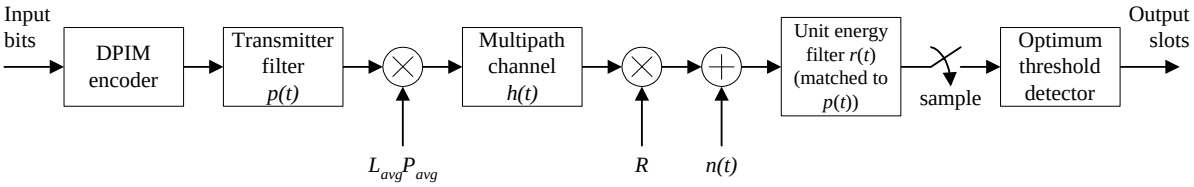

(b)

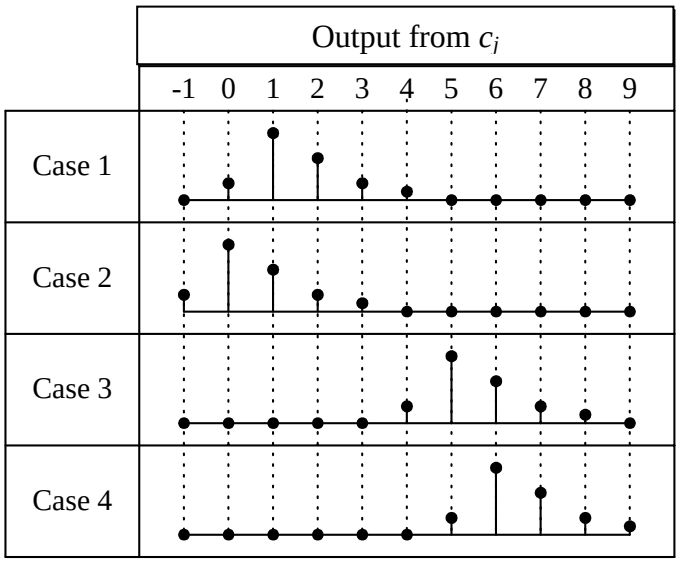
Output from c_i
-1 0 1 2 3 4 5 6 7 8 9
Case 1
Case 2
Case 3
Case 4

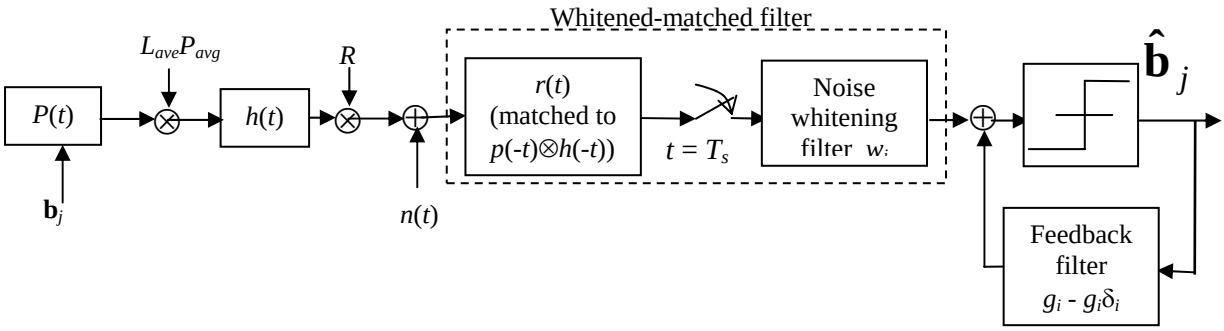
Whitened-matched filter
$L_{ave}P_{avg}$
R
$P(t)$
$h(t)$
$r(t)$
(matched to
$p(-t)\otimes h(-t)$)
$t = T_s$
Noise
whitening
filter w_i
$\hat{\mathbf{b}}_j$
$\mathbf{b}_j$
$n(t)$
Feedback
filter
$g_i - g_i\delta_i$

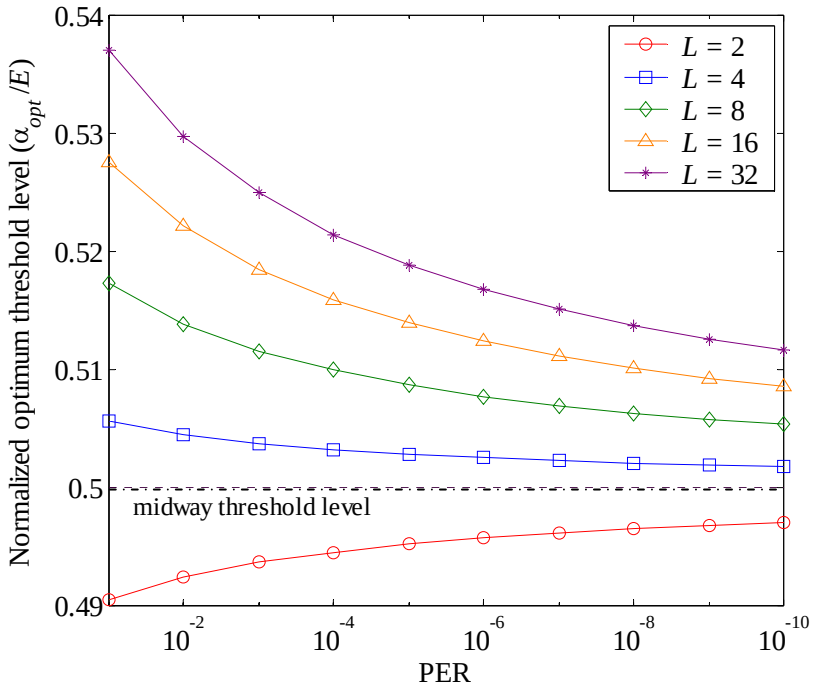
0.54
0.53
0.52
0.51
0.5
0.49
Normalized optimum threshold level (α_{opt}/E)
L = 2
L = 4
L = 8
L = 16
L = 32
midway threshold level
10^{-2}
10^{-4}
10^{-6}
10^{-8}
10^{-10}
PER

(a)

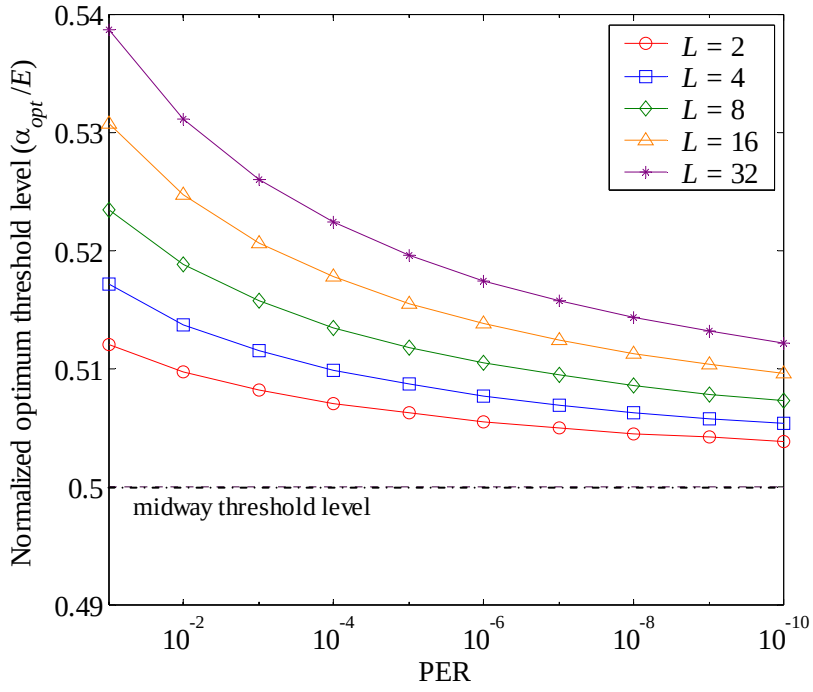
0.54
0.53
0.52
0.51
0.5
0.49
Normalized optimum threshold level (α_{opt}/E)
L = 2
L = 4
L = 8
L = 16
L = 32
midway threshold level
10^{-2}
10^{-4}
10^{-6}
10^{-8}
10^{-10}
PER

(b)

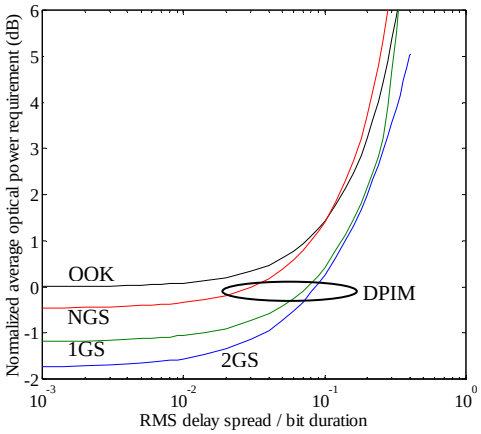
Normalized average optical power requirement (dB)
RMS delay spread / bit duration
OOK
NGS
1GS
2GS
DPIM

(a)

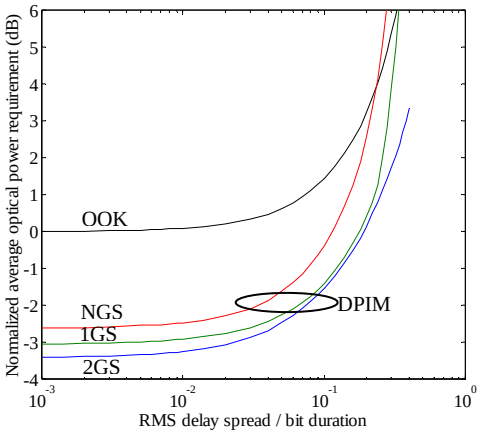
Normalized average optical power requirement (dB)
RMS delay spread / bit duration
OOK
NGS
1GS
2GS
DPIM

(b)

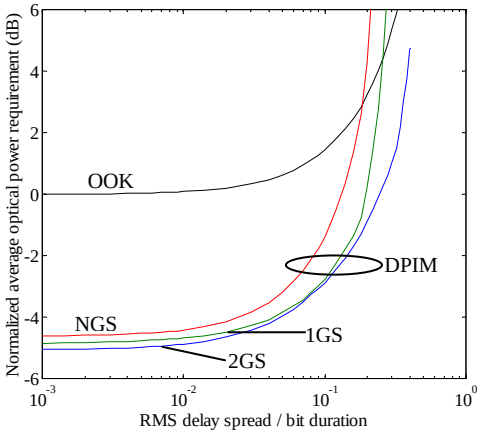
Normalized average optical power requirement (dB)
RMS delay spread / bit duration
OOK
NGS
1GS
2GS
DPIM

(c)

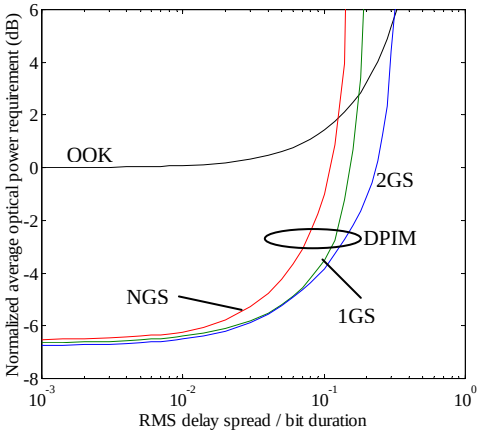
Normalized average optical power requirement (dB)
RMS delay spread / bit duration
OOK
NGS
1GS
2GS
DPIM

(d)

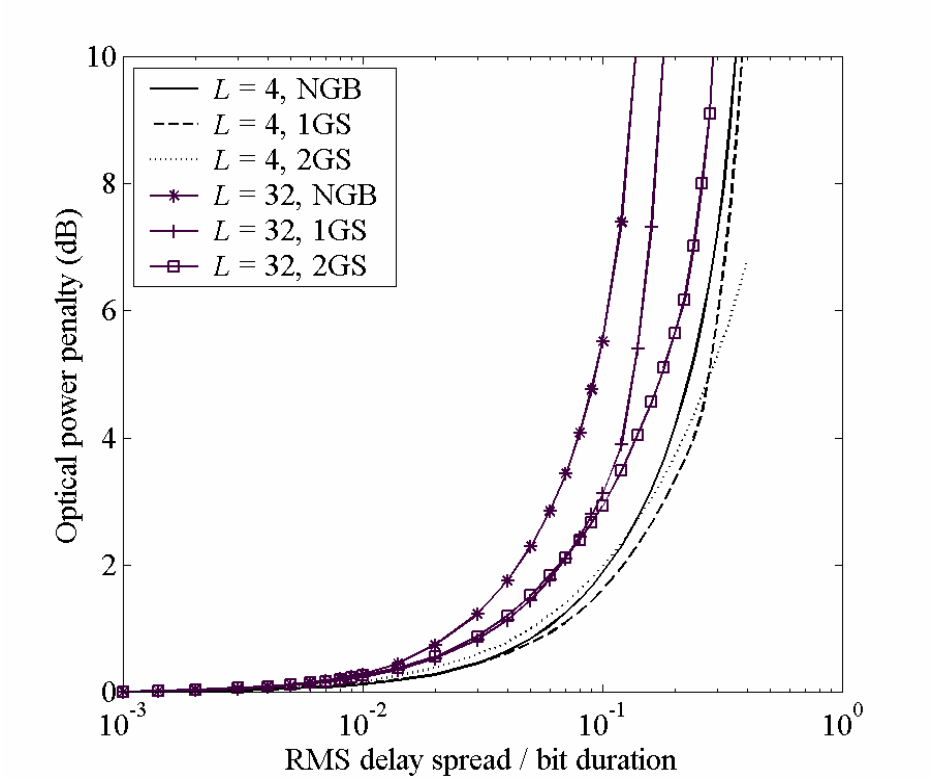
L = 4, NGB
L = 4, 1GS
L = 4, 2GS
L = 32, NGB
L = 32, 1GS
L = 32, 2GS
Optical power penalty (dB)
RMS delay spread / bit duration
0
2
4
6
8
10
10^-3
10^-2
10^-1
10^0

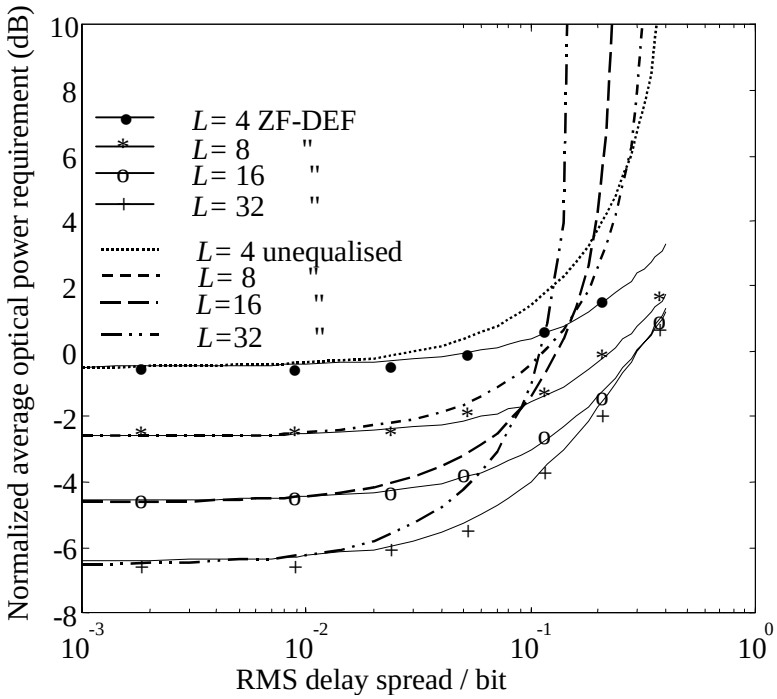
Normalized average optical power requirement (dB)
RMS delay spread / bit
L= 4 ZF-DEF
L= 8 "
L= 16 "
L= 32 "
L= 4 unequalised
L= 8 "
L=16 "
L=32 "
10
8
6
4
2
0
-2
-4
-6
-8
10^-3
10^-2
10^-1
10^0

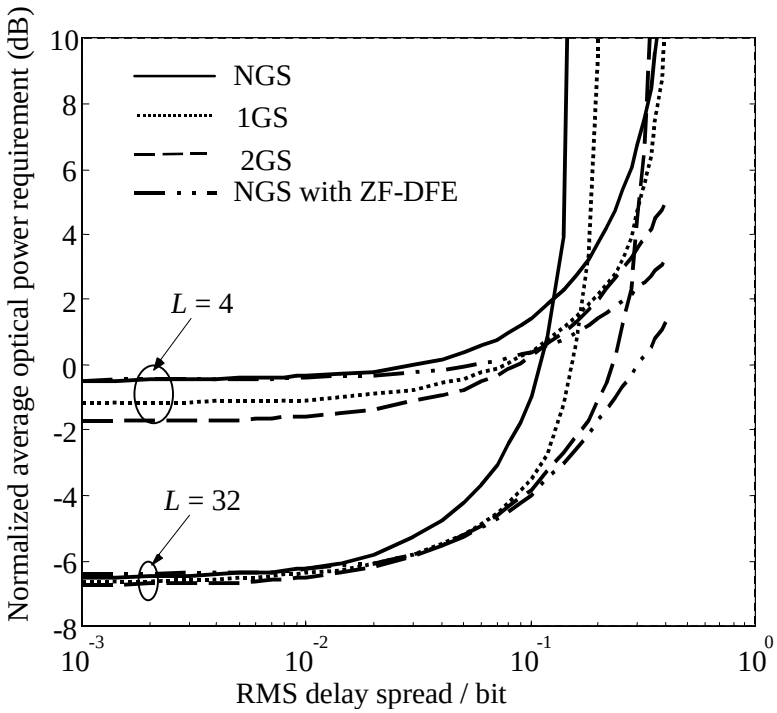
Normalized average optical power requirement (dB)
10
8
6
4
2
0
-2
-4
-6
-8
NGS
1GS
2GS
NGS with ZF-DFE
L = 4
L = 32
10^-3
10^-2
10^-1
10^0
RMS delay spread / bit